Biochimica et Biophysica Acta 1807 (2011) 437–443

Contents lists available at ScienceDirect

Biochimica et Biophysica Acta

journal homepage: www.elsevier.com/locate/bbabio

First solid-state NMR analysis of uniformly ^{13}C-enriched major light-harvesting complexes from *Chlamydomonas reinhardtii* and identification of protein and cofactor spin clusters

Anjali Pandit [a,*], Tomas Morosinotto [b], Michael Reus [c], Alfred R. Holzwarth [c], Roberto Bassi [d], Huub J.M. de Groot [a]

[a] Leiden Institute of Chemistry, Leiden University, PO Box 9502, 2300 RA Leiden, The Netherlands
[b] Department of Biology, Biology Complex "A. Vallisneri"–Piano VI Nord, stanza 60 Via Ugo Bassi 58 B, 35121 Padova, Italy
[c] Max-Planck-Institut für Bioanorganische Chemie, Stiftstrasse 34–36/D-45470 Mülheim an der Ruhr, Germany
[d] Laboratory of Photosynthesis, Department of Biotechnology, University of, Verona University, Strada Le Grazie 15 Verona, 37134 Italy

ARTICLE INFO

Article history:
Received 17 November 2010
Received in revised form 13 January 2011
Accepted 18 January 2011
Available online 26 January 2011

Keywords:
Photosynthetic light-harvesting
Non-photochemical quenching
lhc2 complex
Magic-angle spinning NMR

ABSTRACT

The light-harvesting complex II (LHCII) is the main component of the antenna system of plants and green algae and plays a major role in the capture of sun light for photosynthesis. The LHCII complexes have also been proposed to play a key role in the optimization of photosynthetic efficiency through the process of state 1–state 2 transitions and are involved in down-regulation of photosynthesis under excess light by energy dissipation through non-photochemical quenching (NPQ). We present here the first solid-state magic-angle spinning (MAS) NMR data of the major light-harvesting complex (LHCII) of *Chlamydomonas reinhardtii*, a eukaryotic green alga. We are able to identify nuclear spin clusters of the protein and of its associated chlorophyll pigments in ^{13}C–^{13}C dipolar homonuclear correlation spectra on a uniformly ^{13}C-labeled sample. In particular, we were able to resolve several chlorophyll 13^1 carbon resonances that are sensitive to hydrogen bonding to the 13^1-keto carbonyl group. The data show that ^{13}C NMR signals of the pigments and protein sites are well resolved, thus paving the way to study possible structural reorganization processes involved in light-harvesting regulation through MAS solid-state NMR.

1. Introduction

Solid-state NMR is becoming increasingly important for understanding the structure–function mechanisms of photosynthetic membrane proteins in terms of concerted structural and electronic interactions. Through this technique, the electronic structures of the bacteriochlorophyll (BChl) cofactors and their coordinating histidines in purple bacterial photosynthetic antenna complexes and reaction centers have been determined, as well as the electronic structure of the reaction center primary electron donor in the ground and radical cation states [1–5]. Analysis of the protein NMR chemical shifts in a bacterial light-harvesting 2 complex (LH2) revealed local structural and electronic perturbations of the protein backbone and BChl-coordinating histidine, arising from strain induced by the rigid packing in the pigment–protein oligomer [6,7].

The advantage of solid-state NMR for study of functional photosynthetic architectures is that large membrane proteins can be studied under various sample conditions, ranging from detergent-solubilized protein complexes to large protein aggregates. However, the (partial) assignment of membrane proteins by solid-state NMR is still very challenging with only few examples available up to date [8–12]. This is also due to the fact that eukaryotic systems are often too costly or not easily accessible for this technique in terms of selective isotope label incorporation. While specific labeling with ^{15}N has been successfully applied to Photosystem II from spinach [13], NMR resonance assignments require more abundant labeling strategies, which are prohibitively expensive. No attempt has been made so far to characterize the light-harvesting complexes of higher plants and photosynthetic green algae by solid-state NMR. Yet, there is an urgent need for obtaining more structural information on these pigment–protein complexes, since their light-harvesting proteins play a crucial role not only in photosynthesis itself but also in the mechanisms of regulation and photoprotection including, e.g., state transitions and non-photochemical quenching (NPQ) where conformational changes of the proteins have been proposed [14]. The molecular mechanism of energy dissipation in NPQ in particular is under much debate and is one of the major topics in photosynthesis that remains to be resolved. Several mechanisms have been proposed for the associated reversible switch in pigment configuration, based on protein conformational changes, aggregation-

* Corresponding author at: Present address: Faculty of Sciences, VU University Amsterdam, De Boelelaan 1081 HV Amsterdam, The Netherlands. Tel.: +31 20 5987937; fax: +31 20 5987899.
E-mail address: apandit@few.vu.nl (A. Pandit).

0005-2728/$ – see front matter © 2011 Elsevier B.V. All rights reserved.
doi:10.1016/j.bbabio.2011.01.007

induced surface contacts and/or cofactor exchange [15–23]. Structural tools to detect sensitively the possible conformation changes of these complexes both *in vitro* and *in vivo* are however still missing.

In this paper, we report the first NMR results on uniformly ^{13}C labeled LHCII complexes purified from the green algae *Chlamydomonas reinhardtii* and the perspectives for more in-depth studies on the structural flexibility of oxygenic photosynthetic light-harvesting complexes. The green algae *C. reinhardtii* is one of the most intensely studied eukaryotic algae and its whole genome has been sequenced [24]. The major antenna of the Photosystem II in *C. reinhardtii*, called LHCII, is assembled in trimers and encoded 10 different genes called Lhcbm1–10 [25,26]. Each monomer subunit comprises an apoprotein of ~235 amino acids whose sequences are very well conserved except for the 10–15 residues at the N-terminus. Pigment–protein subunits also include eight chlorophyll *a* (Chl *a*), six Chl *b* and four carotenoids, which have been identified as two luteins and one neoxanthin in the crystal structures of LHCII of pea and spinach [22,27]. The fourth carotenoid, a violaxanthin, is peripherally bound and is easily lost upon protein isolation. *Chlamydomonas* LHCII also contains sub-stoichiometric amounts of the α-carotene derived xanthophyll loroxanthin [28].

We have collected 2D ^{13}C–^{13}C homonuclear correlation spectra of uniformly ^{13}C-labeled *Chlamydomonas* LHCII, showing the feasibility of solid-state NMR to determine structural properties of the Lhcbm proteins as well as the ground-state electronic features of the antenna pigments. The quality of the obtained NMR data is comparable to chemical shift data that were earlier obtained from purple bacterial light-harvesting complexes. For these light-harvesting systems, we could determine the electronic structures of the BChl pigments and we have shown that the NMR chemical shifts are sensitive to localized strain induced by the pigment–protein packing. The results presented here give good perspectives that by specific or site-selective isotope labeling, such atomic-level mechanistic and electronic effects are also detectable in oxygenic antenna complexes of plants and green algae. This gives new perspectives to investigate protein conformational changes associated with light-harvesting regulation and accompanied changes in the pigment ground-state electronic structures.

2. Materials and methods

2.1. Isolation of ^{13}C-labeled thylakoids

C. reinhardtii cells were grown in TAP medium [29], pH-value = 7.0, using ^{13}C-labeled Na-acetate instead of acetic acid as the only carbon source, under illumination with 40 W fluorescence light bulbs in 500 ml flask under regular shaking. In order to achieve maximum labeling at a minimal consumption of ^{13}C-label in a first step, a small amount of cells, taken from a normal culture grown under regular CO_2 supply, has been transferred to unlabeled Na-acetate TAP growth medium in order to adapt the cells to growth without CO_2 supply. After 3 days of growth the cells were then diluted 1:10 with TAP medium containing ^{13}C-labeled Na-acetate as the carbon source. Cells were harvested by centrifugation after 3 days in the upper third of the log-growth phase. Further handling occurred under green safety light in the cool room. The cells were suspended in a ca. 30 ml volume of HEPES 1 buffer and were broken in the cooled French press (200 psi nitrogen). The resulting solution was centrifuged (10,000 rpm in JA-20 rotor) for 10 min. The pellet was suspended in HEPES 2 buffer and the suspension was repelleted at 20,000 rpm in the same rotor for 10 min. The resulting pellet which contained the labeled thylakoids was resuspended in HEPES 3 buffer and was adjusted to a chlorophyll concentration of 2 mg/ml. The samples were subsequently shock frozen in liquid nitrogen.

Used buffers were as follows: HEPES 1: 25 mM Hepes, pH 7.5, 5 mM $MgCl_2$, 0.3 M sucrose; HEPES 2: 25 mM Hepes, pH 7.5, 10 mM Na-EDTA, 0.3 M sucrose; HEPES 3: 25 mM Hepes pH 7.5, 5 mM EDTA, 0.58 M sucrose. All buffers contained the following protease inhibitors: 0.2 mM benzamidinium-hydrochloride, 1 mM amino-capronic acid, 0.2 mM phenyl methane sulfonyl fluoride (PMSF).

2.2. LHCII isolation

Purification of the LHCII complexes from thylakoids has been performed by sucrose gradient centrifugation after solubilization of thylakoids membranes with 0.8% β-DM, as in Caffarri et al. [30]. Trimeric complexes have been then concentrated up to 100 mg/ml, considering protein and pigments together.

2.3. NMR measurements

2D ^{13}C–^{13}C proton driven spin diffusion (PDSD) and radio-frequency driven dipolar recoupling (RFDR) homonuclear correlation spectra of isolated LHCII complexes were collected on a Bruker AV-750 NMR spectrometer (Bruker GmbH, Karlsruhe, Germany) of 17.4 T (^1H frequency 750 MHz) equipped with a triple MAS resonance probe. The LHCII sample contained ~15 mg of protein loaded in a 4 mm CRAMPS rotor and was stepwise cooled to 223 K during slow spinning. Spectra were collected with various mixing times, varying from 50 to 500 ms for the PDSD spectra and from 1 to 5 ms for the RFDR spectra, with a spinning frequency of 13 kHz. The PDSD spectra

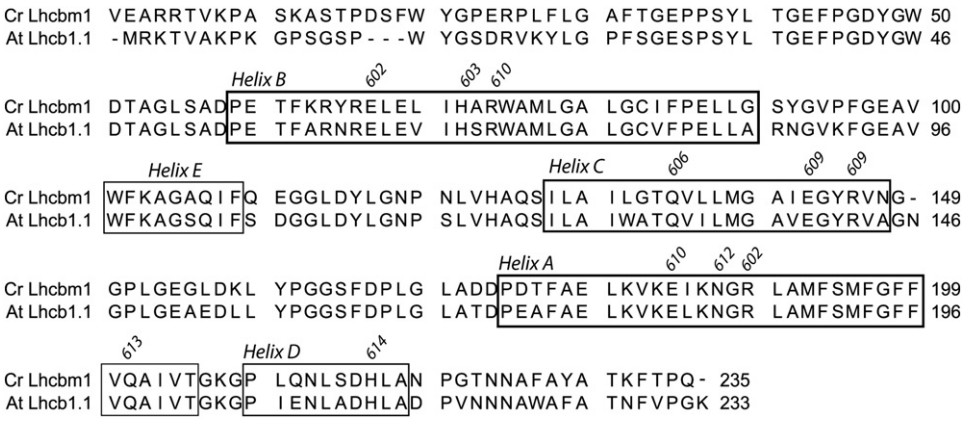

Fig. 1. The Lhcmb1 mature protein sequence from *Chlamydomonas reinhardtii* (Cr) was aligned with Lhcb1.1 from *Arabidopsis thaliana* (At). Helices A–E were identified according to Liu et al. [27]. Chl binding residues are indicated by the numbers of the corresponding Chls in the crystal structure of spinach LHCII and were identified according to Liu et al. and Remelli et al. [27,40].

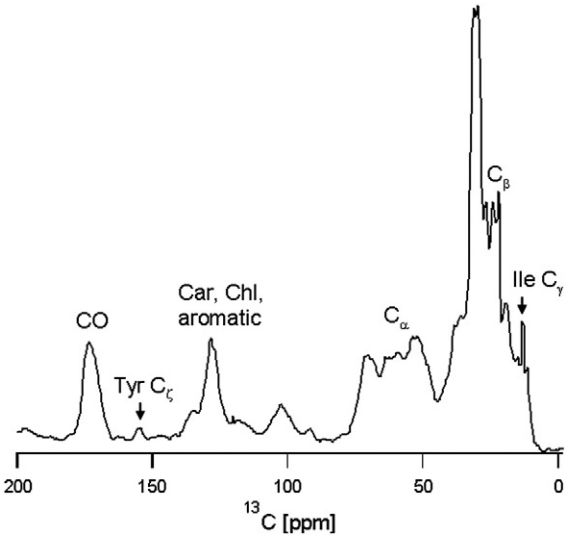

Fig. 2. 1D ^{13}C CP-MAS spectrum of the *Chlamydomonas* LHCII sample. The data were collected in 2000 scans with a MAS rotation frequency of 13 kHz.

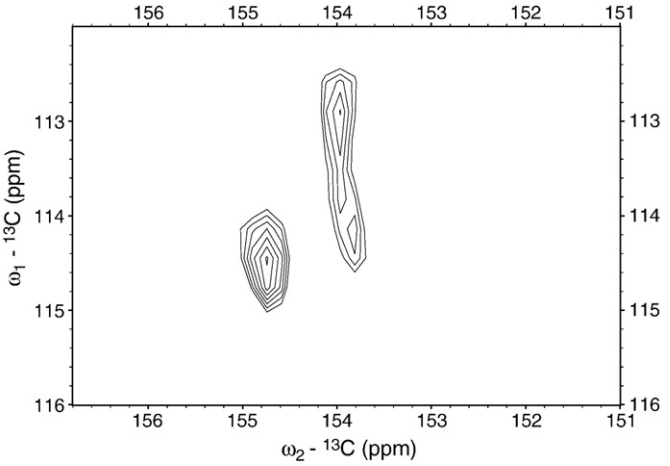

Fig. 4. *Chlamydomonas* LHCII PDSD 2D ^{13}C–^{13}C correlation spectrum acquired at 50 ms mixing time, showing the tyrosine $C_{\varepsilon 1,\varepsilon 2}$–$C_{\zeta}$ cross peaks.

with 500 ms mixing time allowed distinction of inter-residue long-range interactions. The proton 90° pulse was set to 3.1 μs. Two-pulse phase modulation (TPPM) decoupling was applied during the t_1 and t_2 periods [31]. In the RFDR experiment, Rotor-synchronized π-pulses with a length of 8.4 μs were applied during the mixing time. In the t_2 dimension, 2 K data points with a sweep width of 50 kHz were recorded. Zero filling to 4 K and an exponential line broadening of 25 Hz was applied prior to Fourier transformation. In the t_1 dimension, 256 scans using 1 K data points were recorded. For the 1D CP/MAS NMR spectrum, 2000 scans were recorded. The 2D data were processed with the Topspin software version 2.0 (Bruker) and analyzed by using the program Sparky version 3.100 (T. D. Goddard and D. G. Kneller, University of California, San Francisco). The $^{13}COOH$ resonance of U-[^{13}C,^{15N}]-tyrosine/HCl at 172.1 ppm was used as an

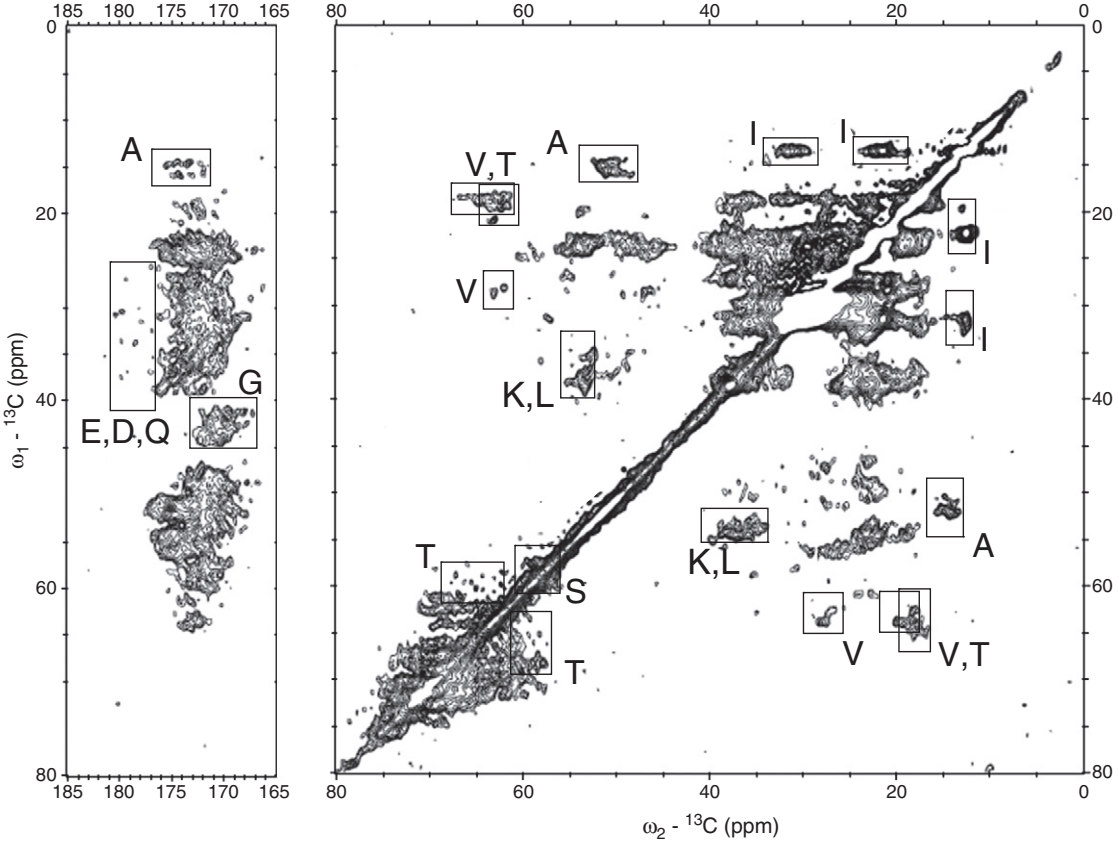

Fig. 3. *Chlamydomonas* LHCII PDSD 2D ^{13}C–^{13}C correlation spectrum of the protein region (0–60 ppm for the C_{α}, C_{β} and side chain resonances and 170–180 ppm for the CO resonances and the rsonances of the negatively-charged side chains) acquired with 50 ms mixing time. The right panel shows the aliphatic region of the 2D spectrum, while the left panel shows the correlations between aliphatic and carbonyl signals.

external chemical shift reference without referencing this standard to tetramethylsilane (TMS) or 4,4-dimethyl-4-silapentane-1-sulfonic acid (DSS).

3. Results and discussion

Fig. 1 shows the Lhcbm1 protein sequence *of C. reinhardtii* and its homology to the Lhcb1.1 sequence of *Arabidopsis thaliana*. The 1D ^{13}C CP-MAS NMR spectrum is presented in Fig. 2. The region from 0 to 70 ppm and the broad peak around 173 ppm contain the protein backbone resonances: the C_β resonances are located around 25–50 ppm, the C_α resonances around 50–70 ppm and the carbonyl resonances around 173 ppm. The large peak around 30 ppm probably arises from lipids that remain associated to the protein complex during isolation. The region around130 ppm contains the aromatic amino acid residues together with the pigment Chl and Car resonances. The Tyr C_ζ and the Ile C_γ peaks are indicated in the spectrum.

3.1. LHCII ^{13}C–^{13}C spectrum—the protein region

Fig. 3 shows the two-dimensional ^{13}C–^{13}C homonuclear PDSD correlation MAS NMR spectrum obtained with 50 ms mixing time. We are able to identify spin clusters of the alanines C_α–C_β (A), glycines C–C_α (G), isoleucines C_β–$C_{\gamma1}$ and $C_{\gamma1}$–$C_{\gamma2}$ (I), valines C_α–C_β and C_β–C_γ (V) and threonines C_α–C_β (T). The broad clusters of the threonine resonances represent the different environments of the threonines, of which some reside in the large loop regions of the protein. In contrast, the isoleucine resonances that reside in the more homogeneous transmembrane alpha-helical part of the protein (see Fig. 1) are clustered in a narrow region. In the CO region around 173 ppm, cross peaks are distinguished of the negatively-charged side chains glutamic acid (Glu) C_δ, aspartic

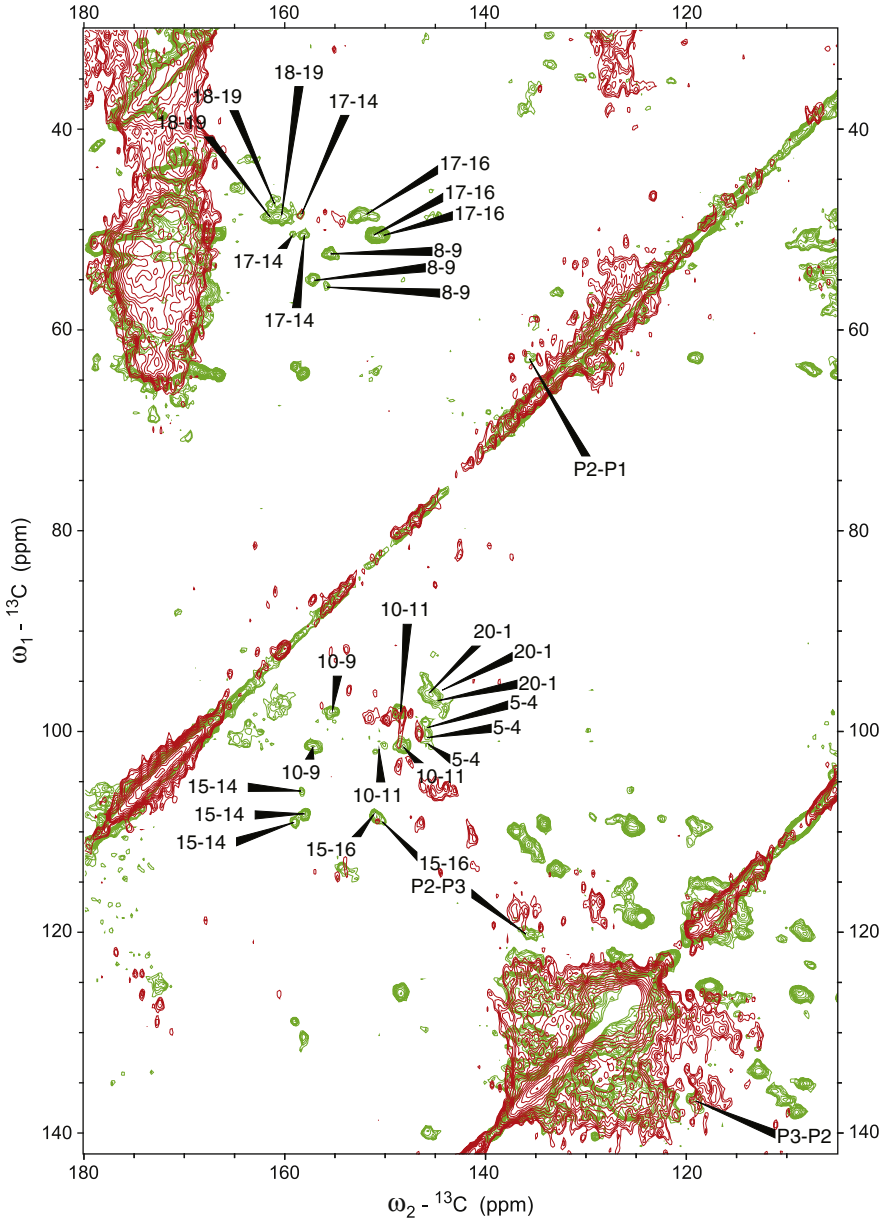

Fig. 5. *Chlamydomonas* LHCII PDSD 2D ^{13}C–^{13}C correlation spectrum acquired with 50 ms mixing time, of the aromatic region in which Chl resonances are observed. The *Chlamydomonas* LHCII spectrum (in red) is overlaid on an RFDR ^{13}C–^{13}C correlation spectrum obtained of the purple bacterial light-harvesting complex 2 of *Rps. acidophila* (in green) of which the BChl ^{13}C resonances have been assigned. In the spectra, also tyrosine side chain resonances are resolved that are presented more clearly in Fig. 4.

acid (Asp) C_γ and glutamine (Gln) C_δ (E, D, Q). The Glu and Gln side chains are involved in Chl H-bonding and coordination, forming the central ligands to several of the Chls in the LHCII complexes of pea and spinach [22,27]. The negatively-charged residues are also possible reporters of a change in pH gradient and may trigger regulatory conformational changes [32]. The narrow line widths of the isolated peaks (~ 0.8 ppm) indicate that, similar to the purple bacterial LH2 antenna protein that was studied extensively by solid-state NMR, the LHCII proteins solubilized in detergent are well-folded, rigid complexes.

In the aromatic region, cross peaks from Chl pigments are observed, and some aromatic side chains of the protein can be identified. The tyrosine (Tyr) side chain C_ε–C_ζ cross peaks are resolved, since their position is also well-separated from other resonances. Fig. 4 presents the resolved Tyr C_ε–C_ζ cross resonances that fall into three cross peaks (C_ζ = 153.8, 153.9 and 154.7 ppm with respective volumes of 30%, 26% and 44%). All Lhcbm apoproteins contain at least 6 Tyr residues (Fig. 1) that occur in the loop regions of the protein with heterogeneity of the protein environments. None of the tyrosine resonances are shifted downfield towards the values for tyrosinate.

3.2. LHCII ^{13}C–^{13}C spectrum—the pigment region

In Fig. 5, the two-dimensional ^{13}C–^{13}C homonuclear correlation MAS NMR data of LHCII for the aromatic region (drawn in red) are overlaid on a spectrum of the purple bacterial light-harvesting 2 complex for *Rhodopseudomonas acidophila* (LH2, drawn in green), for which a complete assignment of its bacteriochlorophylls (BChls) has been obtained previously [5]. Overlay of the spectrum of LHCII on the spectrum of the purple bacterial LH2 allows a comparison of the local environments of the pigments in the two types of complexes, related to their optical spectroscopic properties. By similar "homology mapping" of the spectra of purple bacterial core (LH1) on the one hand and bacterial peripheral (LH2) antenna complexes on the other hand, the differences in their BChl electronic structures were directly compared [3]. More variety is expected comparing the ^{13}C responses of the Chl pigments of *Chlamydomonas* LHCII and *Rps. acidophila* LH2, due to the structural differences in their pigment–protein assemblies. The crystal structures of trimeric LHCII and of the LH2 complex of *Rps. acidophila* are shown in Fig. 6. Whereas the LHCII complexes are assembled in trimers of which each monomer contains 14 Chls (depicted in green in Fig. 6A), the LH2 peripheral antenna complex of the purple bacterium *Rps. acidophila* is a ring-shaped nonamer complex, in which each of the nine subunits contains three BChls (in green in Fig. 6B). Two BChls in the LH2 subunit form a dimer and the LH2 oligomer complex contains a ring of BChl dimers that are excitonically coupled.

The LH2 BChl ^{13}C–^{13}C resonances are labeled in the green spectrum in Fig. 5. The three BChls per subunit reside in different protein environments and have three distinctive sets of ^{13}C chemical shifts. Evidently the LH2 nonamer complex is structurally very homogeneous resulting in nine identical spin signals collected for each of the three subunit BChls, yielding a high S/N ratio. Compared to the LH2 BChl signals, the LHCII Chl signals are weaker and have lower S/N ratios. This can be explained by heterogeneity of the pigment–protein environments of the LHCII antennae that are more disordered structures than LH2. If the 14 Chls per monomer reside in different protein environments – as is suggested by the LHCII crystal structures [22,27] and by the differences in their site energies [33] – their ^{13}C resonances will not overlap. For each Chl, in this way only three spin signals are collected per LHCII trimer complex, resulting in a lower S/N per mole protein.

In the lower part of the spectrum in Fig. 5, some of the resonance cross peaks observed for the LHCII complex (in red) coincide with the LH2 resonances (in green). Relying on the LH2 BChl assignments, few Chl signals are tentatively assigned. In the LHCII spectrum the cross peak at 100.3–146.6 ppm is tentatively attributed to the Chl C4-5 resonances and the cross peak at 109.0–150.0 ppm to the Chl C15–16 resonances. A large number of LHCII signals occur in the region of the LH2 BChl C10–11 cross peaks (ω1: 95–105 ppm, ω2: 147–153 ppm) that could be due to heterogeneity of the LHCII Chl C10–11 resonances and/or overlap of the C10–11 and C5-4 cross signals. Overall, many LHCII cross signals deviate from the signals of the LH2 BChls, which could represent differences in the LHCII Chl and LH2 BChl protein surroundings. In this stage, we cannot attribute any Chl signals to specific Chls in the structure.

The cross resonances of the Car phytyl groups are all clustered in the narrow region of 120–140 ppm in the lower right part of the spectrum in Fig. 5, while the Car head group signals fall in the region that is dominated by the protein signals (30–60 ppm) [34]. Assignment of the Car signals would require a more extended study that includes Car-specific isotope labeling and performing experiments at higher magnetic fields for better separation.

Fig. 7 shows the Chl $C13^2$–$C13^1$ cross peaks that are easily resolved owing to their position in an isolated part of the spectrum. The LHCII spectrum (in red) again is overlaid on the RFDR spectrum of *acidophila* LH2 (in green). The Chl *a* and Chl *b* $C13^1$ keto carbonyls are capable of hydrogen bonding. The H-bonding patterns of LHCII Chls depend on the oligomerized state of the complexes, associated with their *in vitro*

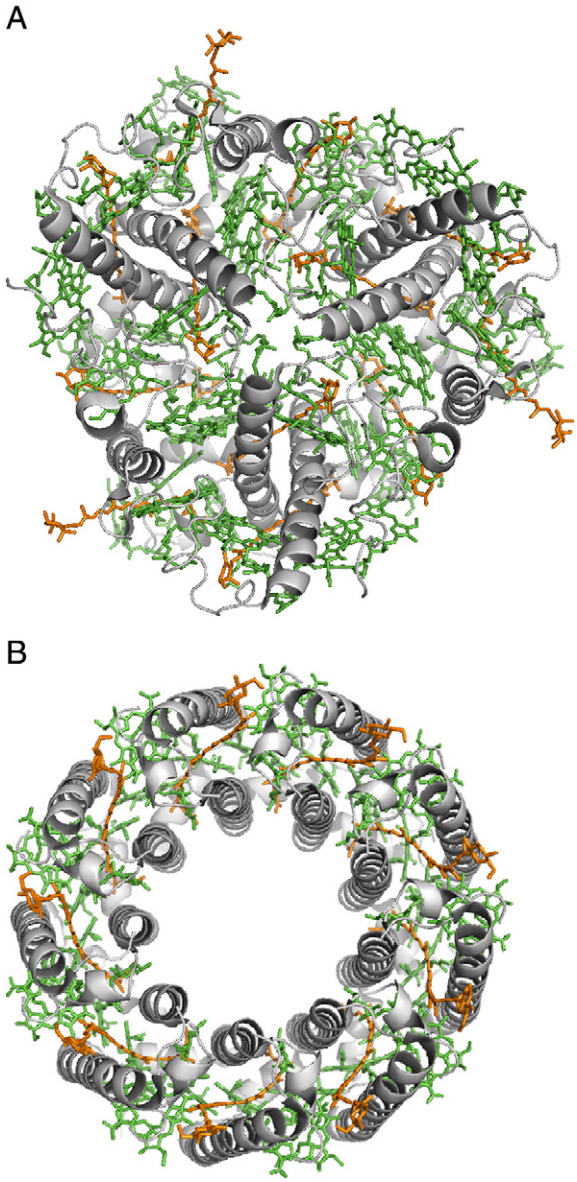

Fig. 6. (A) The crystal structure of trimeric LHCII (PDB ID: 2bhw) and (B) the crystal structure of LH2 of *Rps. acidophila* (PDB ID: 2fkw). The (bacterio)chlorophylls are colored in green and the carotenoids in orange.

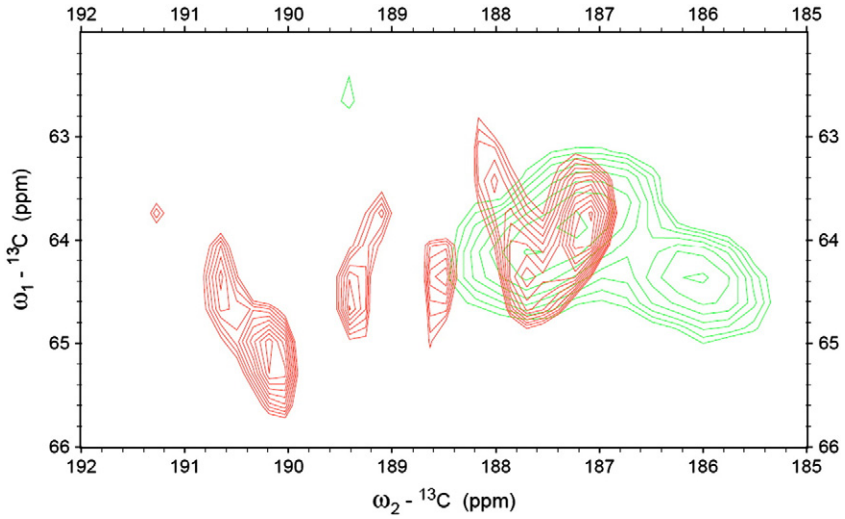

Fig. 7. *Chlamydomonas* LHCII PDSD ^{13}C–^{13}C correlation spectrum (in red) acquired at 50 ms mixing time, showing the diversity in the Chl 13^2–13^1 resonances. The spectrum is overlaid on an RFDR ^{13}C–^{13}C correlation spectrum obtained of the purple bacterial light-harvesting complex 2 of *Rps. acidophila* (in green), which shows three distinctive 13^2–13^1 cross resonances for the three types of LH2 BChls (B850α, B850β and B800).

fluorescence quenching characteristics. Resonance Raman experiments on detergent-solubilized trimeric LHC II, as was used in this study, and highly oligomerized plant LHCII complexes revealed that during the oligomerization process an H-bond is formed to a Chl *b* formyl group and to a Chl *a* keto carbonyl group [35].

Table 1 presents the resolved $C13^1$ resonances and their shifts relative to the $C13^1$ resonances of monomeric BChl in acetone-d_6 [5] that were obtained in an earlier study using the same reference (note that BChl and Chl $C13^1$ keto carbonyl side chain structures are identical so that they can be compared). The Chl resonances fall into eight cross peaks with different relative intensities. The Chl **ii** line is relatively broad and the intensity is relatively strong, suggesting that the signals arise from several chromophores. In contrast, the response of Chl **iii** is very narrow and the keto carbonyl side chain of this chromophore should be in a very rigid position. Formation of a hydrogen bond to the Chl keto carbonyl can downshift the $C13^1$ resonances compared to the chromophore in solution. According to Table 1 this might be the case for 25–35% of the Chls (i.e., 3–5 Chls assuming that the signals arise from fourteen different Chls in total). This roughly estimated number should be taken with some caution since the relative intensities of the NMR signals can be affected by different factors. The number is smaller than for the LHCII structure from spinach, where 6 out of the 14 Chls have H-bonded keto carbonyls [27].

4. Conclusions

The resolution of the 2D NMR spectra that we obtained for uniformly ^{13}C labeled LHCII antennae is sufficient to identify pigment and protein spin clusters, including residues that are possibly involved in the regulatory role of light-harvesting. This is important, because it implies that we have a structural tool to monitor light-regulated structural changes in detail even in uniformly labeled samples. In particular, the Chl 13^1 resonances that are sensitive to H-bonding and associated environmental changes in different aggregation states are easily resolved in the LHCII 2D NMR spectrum. The narrow NMR lines show that the LHCII complex also forms a very ordered structure under non-crystalline conditions. The comparison of the LHCII Chl signals to the LH2 BChl signals illustrates how the structural heterogeneity of different antennae is reflected in the NMR spectra. This type of "homology mapping" gives a method to compare the pigment local environments of different types of antenna complexes or to compare the pigment environments of an antenna system brought into different functional states.

Extensive NMR studies on a purple bacterial LH2 complex, for which a high-resolution X-ray structure exists [36], have demonstrated that by solid-state NMR we can probe the pigment and protein electronic structures and resolve structural details complementary to X-ray structural data [3,5–7]. The resolution of the collected LHCII NMR spectra in this pilot study suggests that in future experiments such details can also be obtained from plant or green-algae antenna complexes, if site-specific and selective isotope labeling is applied. Intrinsic labeling of the Chls is also possible by addition of ^{13}C-labeled δ-aminolevulinic acid, a precursor for the Chl macrocycles, to the growth medium. This method has successfully been applied to selectively label BChls and bacteriopheophytin (Bpheo) in bacterial photosynthetic reaction centers (see for instance Ref. [4]) and to selectively label Chls in intact cells of cyanobacteria *Synechocystis* [37].

We propose that solid-state NMR techniques applied on oxygenic light-harvesting complexes could be valuable tools to probe mechanistic effects and concerted protein and pigment conformational and electronic changes associated with light-harvesting regulation. New developments to perform high-resolution NMR of proteins in native membranes are promising [38] and may in the future be applicable to study whole thylakoid membranes or "LHCII-only" macrodomains, which consist of arrays of LHCII trimers with similar long range chiral order as the native membranes [39]. This would extend the possibilities of solid-state NMR to probe the structural plasticity of light-harvesting antennae in great detail in a native photosynthetic membrane.

Table 1
Chlorophyll ^{13}C keto carbonyl assignments and relative shifts $\Delta\sigma$ compared to monomeric BChl *a* in acetone [5].

Chl	$C13^1$ [ppm]	$\Delta\sigma 13^1$ [ppm]	Line width [Hz]	Rel. volume [%]
i	187.0	−2.0	137.0	12
ii	187.7	−1.3	196.4	23
iii	188.0	−1.0	96.8	9.8
iv	188.5	−0.5	150.8	13
v	189.1	+0.1	149.4	6.7
vi	189.4	+0.4	139.4	10.9
vii	190.2	+1.2	155.7	14
viii	190.7	+1.7	134.0	9.8

References

[1] A. Alia, J. Matysik, I. de Boer, P. Gast, H.J. van Gorkom, H.J.M. de Groot, Heteronuclear 2D (1H-13C) MAS NMR resolves the electronic structure of coordinated histidines in light-harvesting complex II: assessment of charge transfer and electronic delocalization effect, J. Biomol. NMR 28 (2004) 157–164.

[2] E. Daviso, S. Prakash, A. Alia, P. Gast, J. Neugebauer, G. Jeschke, J. Matysik, The electronic structure of the primary electron donor of reaction centers of purple bacteria at atomic resolution as observed by photo-CIDNP 13C NMR, Proc. Natl Acad. Sci. USA 106 (2009) 22281–22286.

[3] A. Pandit, F. Buda, A.J. van Gammeren, S. Ganapathy, H.J.M. de Groot, Selective chemical shift assignment of bacteriochlorophyll a in uniformly [C-13-N-15]-labeled light-harvesting 1 complexes by solid-state NMR in ultrahigh magnetic field, J. Phys. Chem. B 114 (2010) 6207–6215.

[4] S. Prakash, A. Alia, P. Gast, H.J.M. de Groot, G. Jeschke, J. Matysik, C-13 chemical shift map of the active cofactors in photosynthetic reaction centers of *Rhodobacter* sphaeroides revealed by photo-CIDNP MAS NMR, Biochemistry 46 (2007) 8953–8960.

[5] A.J. van Gammeren, F. Buda, F.B. Hulsbergen, S. Kiihne, J.G. Hollander, T.A. Egorova-Zachernyuk, N.J. Fraser, R.J. Cogdell, H.J.M. de Groot, Selective chemical shift assignment of B800 and B850 bacteriochlorophylls in uniformly [C-13, N-15]-labeled light-harvesting complexes by solid-state NMR spectroscopy at ultra-high magnetic field, J. Am. Chem. Soc. 127 (2005) 3213–3219.

[6] A. Pandit, P.K. Wawrzyniak, A.J. van Gammeren, F. Buda, S. Ganapathy, H.J.M. de Groot, Nuclear magnetic resonance secondary shifts of a light-harvesting 2 complex reveal local backbone perturbations induced by its higher-order interactions, Biochemistry 49 (2010) 478–486.

[7] P.K. Wawrzyniak, A. Alia, R.G. Schaap, M.M. Heemskerk, H.J.M. de Groot, F. Buda, Protein-induced geometric constraints and charge transfer in bacteriochlorophyll–histidine complexes in LH2, Phys. Chem. Chem. Phys. 10 (2008) 6971–6978.

[8] L.C. Shi, M.A.M. Ahmed, W.R. Zhang, G. Whited, L.S. Brown, V. Ladizhansky, Three-dimensional solid-state NMR study of a seven-helical integral membrane proton pump-structural insights, J. Mol. Biol. 386 (2009) 1078–1093.

[9] L. Huang, A.E. McDermott, Partial site-specific assignment of a uniformly C-13, N-15 enriched membrane protein, light-harvesting complex 1 (LH1), by solid state NMR, Biochim. Biophys. Acta-Bioenerg. 1777 (2008) 1098–1108.

[10] K. Varga, L. Tian, A.E. McDermott, Solid-state NMR study and assignments of the KcsA potassium ion channel of *S. lividans*, BBA-proteins, Proteomics 1774 (2007) 1604–1613.

[11] A. Goldbourt, B.J. Gross, L.A. Day, A.E. McDermott, Filamentous phage studied by magic-angle spinning NMR: resonance assignment and secondary structure of the coat protein in Pf1, J. Am. Chem. Soc. 129 (2007) 2338–2344.

[12] A. Loquet, B. Bardiaux, C. Gardiennet, C. Blanchet, M. Baldus, M. Nilges, T. Malliavin, A. Bockmann, 3D structure determination of the Crh protein from highly ambiguous solid-state NMR restraints, J. Am. Chem. Soc. 130 (2008) 3579–3589.

[13] A. Diller, E. Roy, P. Gast, H.J. van Gorkom, H.J.M. de Groot, C. Glaubitz, G. Jeschke, J. Matysik, A. Alia, N-15 photochemically induced dynamic nuclear polarization magic-angle spinning NMR analysis of the electron donor of photosystem II, Proc. Natl Acad. Sci. USA 104 (2007) 12767–12771.

[14] S. Eberhard, G. Finazzi, F.A. Wollman, The dynamics of photosynthesis, Annu. Rev. Genet. 42 (2008) 463–515.

[15] T. Barros, A. Royant, J. Standfuss, A. Dreuw, W. Kuhlbrandt, Crystal structure of plant light-harvesting complex shows the active, energy-transmitting state, EMBO J. 28 (2009) 298–306.

[16] A.V. Ruban, R. Berera, C. Ilioaia, I.H.M. van Stokkum, J.T.M. Kennis, A.A. Pascal, H. van Amerongen, B. Robert, P. Horton, R. van Grondelle, Identification of a mechanism of photoprotective energy dissipation in higher plants, Nature 450 (2007) 575–578.

[17] N.E. Holt, D. Zigmantas, L. Valkunas, X.P. Li, K.K. Niyogi, G.R. Fleming, Carotenoid cation formation and the regulation of photosynthetic light harvesting, Science 307 (2005) 433–436.

[18] T.K. Ahn, T.J. Avenson, M. Ballottari, Y.C. Cheng, K.K. Niyogi, R. Bassi, G.R. Fleming, Architecture of a charge-transfer state regulating light harvesting in a plant antenna protein, Science 320 (2008) 794–797.

[19] A.R. Holzwarth, Y. Miloslavina, M. Nilkens, P. Jahns, Identification of two quenching sites active in the regulation of photosynthetic light-harvesting studied by time-resolved fluorescence, Chem. Phys. Lett. 483 (2009) 262–267.

[20] H.A. Frank, J.A. Bautista, J.S. Josue, A.J. Young, Mechanism of nonphotochemical quenching in green plants: energies of the lowest excited singlet states of violaxanthin and zeaxanthin, Biochemistry 39 (2000) 2831–2837.

[21] T. Barros, W. Kuhlbrandt, Crystallisation, structure and function of plant light-harvesting Complex II, Biochim. Biophys. Acta-Bioenerg. 1787 (2009) 753–772.

[22] R. Standfuss, A.C.T. van Scheltinga, M. Lamborghini, W. Kuhlbrandt, Mechanisms of photoprotection and nonphotochemical quenching in pea light-harvesting complex at 2.5A resolution, EMBO J. 24 (2005) 919–928.

[23] M.G. Muller, P. Lambrev, M. Reus, E. Wientjes, R. Croce, A.R. Holzwarth, Singlet energy dissipation in the photosystem II light-harvesting complex does not involve energy transfer to carotenoids, Chem. Phys. Chem. 11 (2010) 1289–1296.

[24] S.S. Merchant, S.E. Prochnik, O. Vallon, E.H. Harris, S.J. Karpowicz, G.B. Witman, A. Terry, A. Salamov, L.K. Fritz-Laylin, L. Marechal-Drouard, W.F. Marshall, L.H. Qu, D.R. Nelson, A.A. Sanderfoot, M.H. Spalding, V.V. Kapitonov, Q.H. Ren, P. Ferris, E. Lindquist, H. Shapiro, S.M. Lucas, J. Grimwood, J. Schmutz, P. Cardol, H. Cerutti, G. Chanfreau, C.L. Chen, V. Cognat, M.T. Croft, R. Dent, S. Dutcher, E. Fernandez, H. Fukuzawa, D. Gonzalez-Balle, D. Gonzalez-Halphen, A. Hallmann, M. Hanikenne, M. Hippler, W. Inwood, K. Jabbari, M. Kalanon, R. Kuras, P.A. Lefebvre, S.D. Lemaire, A.V. Lobanov, M. Lohr, A. Manuell, I. Meir, L. Mets, M. Mittag, T. Mittelmeier, J.V. Moroney, J. Moseley, C. Napoli, A.M. Nedelcu, K. Niyogi, S.V. Novoselov, I.T. Paulsen, G. Pazour, S. Purton, J.P. Ral, D.M. Riano-Pachon, W. Riekhof, L. Rymarquis, M. Schroda, D. Stern, J. Umen, R. Willows, N. Wilson, S.L. Zimmer, J. Allmer, J. Balk, K. Bisova, C.J. Chen, M. Elias, K. Gendler, C. Hauser, M.R. Lamb, H. Ledford, J.C. Long, J. Minagawa, M.D. Page, J.M. Pan, W. Pootakham, S. Roje, A. Rose, E. Stahlberg, A.M. Terauchi, P.F. Yang, S. Ball, C. Bowler, C.L. Dieckmann, V.N. Gladyshev, P. Green, R. Jorgensen, S. Mayfield, B. Mueller-Roeber, S. Rajamani, R.T. Sayre, P. Brokstein, I. Dubchak, D. Goodstein, L. Hornick, Y.W. Huang, J. Jhaveri, Y.G. Luo, D. Martinez, W.C.A. Ngau, B. Otillar, A. Poliakov, A. Porter, L. Szajkowski, G. Werner, K.M. Zhou, I.V. Grigoriev, D.S. Rokhsar, A.R. Grossman, J.G.I.A.T., Chlamydomonas annotation, the *Chlamydomonas* genome reveals the evolution of key animal and plant functions, Science 318 (2007) 245–251.

[25] E.J. Stauber, A. Fink, C. Markert, O. Kruse, U. Johanningmeier, M. Hippler, Proteomics of *Chlamydomonas reinhardtii* light-harvesting proteins, Eukaryot. Cell 2 (2003) 978–994.

[26] D. Elrad, A.R. Grossman, A genome's-eye view of the light-harvesting polypeptides of *Chlamydomonas reinhardtii*, Curr. Genet. 45 (2004) 61–75.

[27] Z.F. Liu, H.C. Yan, K.B. Wang, T.Y. Kuang, J.P. Zhang, L.L. Gui, X.M. An, W.R. Chang, Crystal structure of spinach major light-harvesting complex at 2.72 Angstrom resolution, Nature 428 (2004) 287–292.

[28] K.K. Niyogi, O. Bjorkman, A.R. Grossman, The roles of specific xanthophylls in photoprotection, Proc. Natl Acad. Sci. USA 94 (1997) 14162–14167.

[29] D.S. Gorman, R.P. Levine, Cytochrome F and plastocyanin—their sequence in photosynthetic electron transport chain of chlamydomonas reinhardi, Proc. Natl Acad. Sci. USA 54 (1965) 1665–1669.

[30] S. Caffarri, R. Croce, J. Breton, R. Bassi, The major antenna complex of photosystem II has a xanthophyll binding site not involved in light harvesting, J. Biol. Chem. 276 (2001) 35924–35933.

[31] A.E. Bennet, J.K. Ok, R.G. Griffin, S. Vega, Chemical-shift correlation spectroscopy in rotating solids—radio frequency-driven dipolar recoupling and longitudinal exchange, J. Chem. Phys. 96 (1992) 8624–8627.

[32] C.H. Yang, P. Lambrev, Z. Chen, T. Javorfi, A.Z. Kiss, H. Paulsen, G. Garab, The negatively charged amino acids in the lumenal loop influence the pigment binding and conformation of the major light-harvesting chlorophyll a/b complex of photosystem II, Biochim. Biophys. Acta-Bioenerg. 1777 (2008) 1463–1470.

[33] V.I. Novoderezhkin, M.A. Palacios, H. van Amerongen, R. van Grondelle, Excitation dynamics in the LHCII complex of higher plants: modeling based on the 2.72 Angstrom crystal structure, J. Phys. Chem. B 109 (2005) 10493–10504.

[34] G.P. Moss, C-13 NMR-spectra of carotenoids/oids, Pure Appl. Chem. 47 (1976) 97–102.

[35] A.V. Ruban, P. Horton, B. Robert, Resonance raman-spectroscopy of the photosystem-II light-harvesting complex of green plants—a comparison of trimeric and aggregated, Biochemistry 34 (1995) 2333–2337.

[36] M.Z. Papiz, S.M. Prince, T. Howard, R.J. Cogdell, N.W. Isaacs, The structure and thermal motion of the B800-850 LH2 complex from *Rps. acidophila* at 2.0 (A)over-circle resolution and 100 K: new structural features and functionally relevant motions, J. Mol. Biol. 326 (2003) 1523–1538.

[37] G.J. Janssen, E. Daviso, M. van Son, H.J.M. de Groot, A. Alia, J. Matysik, Observation of the solid-state photo-CIDNP effect in entire cells of cyanobacteria *Synechocystis*, Photosynth. Res. 104 (2010) 275–282.

[38] K. Varga, L. Aslimovska, A. Watts, Advances towards resonance assignments for uniformly—C-13, N-15 enriched bacteriorhodopsin at 18.8T in purple membranes, J. Biomol. NMR 41 (2008) 1–4.

[39] J.K. Holm, Z. Varkonyi, L. Kovacs, D. Posselt, G. Garab, Thermo-optically induced reorganizations in the main light harvesting antenna of plants. II. Indications for the role of LHCII-only macrodomains in thylakoids, Photosynth. Res. 86 (2005) 275–282.

[40] R. Remelli, C. Varotto, D. Sandona, R. Croce, R. Bassi, Chlorophyll binding to monomeric light-harvesting complex—a mutation analysis of chromophore-binding residues, J. Biol. Chem. 274 (1999) 33510–33521.